Developmental Genome-Wide DNA Methylation Asymmetry Between Mouse Placenta and Embryo

Legault LM[1,2], Doiron K[1], Lemieux A[1,2], Caron M[1,3], Chan D[3], Lopes FL[4], Bourque G[5,6,7], Sinnett D[1,8], McGraw S[1,2,9,#].

[1]Research Center of the CHU Sainte-Justine, Montreal, Canada.
[2]Department of Biochemistry and Molecular Medicine, Université de Montréal, Montreal, Canada.
[3]Research Institute of the McGill University Health Centre, Montreal, Quebec, Canada
[4]São Paulo State University (Unesp), School of Veterinary Medicine, Aracatuba, Brazil
[5]Department of Human Genetics, McGill University, Montreal, Quebec, Canada
[6]McGill University and Genome Quebec Innovation Centre, Montreal, Quebec, Canada
[7]Canadian Center for Computational Genomics, Montreal, Quebec, Canada
[8]Department of Pediatrics, Université de Montréal, Montreal, Canada.
[9]Department of Obstetrics and Gynecology, Université de Montréal, Montreal, Canada.

[#]Corresponding author: serge.mcgraw@umontreal.ca

Running title: Embryonic & Placental DNAme Asymmetry

Summary statement: The kinetics of asymmetric DNA methylation acquisition of embryo-placenta differentially methylated regions is not a stepwise process occurring in embryonic and extraembryonic lineages, but a prompt progression in the early post-implanted conceptus.

ABSTRACT

In early embryos, DNA methylation is remodelled to initiate the developmental program but for mostly unknown reasons, methylation marks are acquired unequally between embryonic and placental cells. To better understand this, we generated high-resolution DNA methylation maps of mouse mid-gestation (E10.5) embryo and placenta. We uncovered specific subtypes of differentially methylated regions (DMRs) that contribute directly to the developmental asymmetry existing between mid-gestation embryonic and placental DNA methylation patterns. We show that the asymmetry occurs rapidly during the acquisition of marks in the post-implanted conceptus (E3.5-E6.5), and that these patterns are long-lasting across subtypes of DMRs throughout prenatal development and in somatic tissues. We reveal that at the peri-implantation stages, the *de novo* methyltransferase activity of DNMT3B is the main driver of methylation marks on asymmetric DMRs, and that DNMT3B can largely compensate for lack of DNMT3A in the epiblast and extraembryonic ectoderm, whereas DNMT3A can only partially compensate in the absence of DNMT3B. However, as development progresses and as DNMT3A becomes the principal *de novo* methyltransferase, the compensatory DNA methylation mechanism of DNMT3B on DMRs becomes less effective.

44 **INTRODUCTION**

45 Throughout the eutherian mammalian gestation, the placenta plays an essential role in
46 mediating maternal–embryonic exchanges of gas, nutrients and waste, and also provides the
47 developing embryo with a protective layer against adverse environmental exposures and the
48 maternal immune system (Rossant & Cross, 2001). These unique placental functions are
49 orchestrated by several distinct trophoblast cell subtypes organized in separate layers (Cross,
50 2000). The initial steps of lineage specialization of both placental and embryonic cells occur
51 promptly following fertilization during the first few embryonic cleavages as DNA methylation
52 marks are being reprogrammed (Morgan, Santos, Green, Dean, & Reik, 2005).

53 DNA methylation is an epigenetic mechanism that is critical in the determination of
54 lineage-specific differentiation and development, and is mainly recognized for its involvement in
55 processes such as transcriptional repression, genomic imprinting and X-inactivation (Bestor,
56 2000). DNA methylation marks are mediated by the action of DNA methyltransferases (DNMTs).
57 Establishment of new or *de novo* DNA methylation patterns required for cell lineage determination
58 during development is mediated by DNMT3A and DNMT3B, with cofactor DNMT3L, (Li, 2002;
59 Okano, Bell, Haber, & Li, 1999), whereas DNMT1 maintains heritable DNA methylation patterns
60 during cellular divisions (Lei et al., 1996; Leonhardt, Page, Weier, & Bestor, 1992). These
61 enzymes are critical, as deletion of *Dnmt3b* or *Dnmt1* is embryonic lethal, while *Dnmt3a*-deficient
62 offspring die shortly after birth (Li, Bestor, & Jaenisch, 1992; Okano et al., 1999). During
63 gametogenesis, the acquisition of genome-wide and allele-specific methylation patterns (i.e.
64 genomic imprinting) in both oocytes and sperm is essentially due to the activity of DNMT3A
65 (Kaneda et al., 2004; Kato et al., 2007). Following fertilization, a reprogramming wave removes
66 most methylation signatures across the genome, except for imprinted regions, some types of repeat
67 sequences, as well as imprinted-like sequences, to trigger the developmental program (Hirasawa
68 et al., 2008; Howell et al., 2001; McGraw et al., 2015). Then, during the peri-implantation process,
69 DNA methylation profiles are re-acquired in a sex-, cell- and tissue-specific manner across most
70 parts of the genome by the combined action of DNMT3A and DNMT3B. In the early stages of the
71 *de novo* methylation wave (E4.5-E7.5), the expression of *Dnmt3b* is more robust than *Dnmt3a* in
72 the epiblast and embryonic-derived cells (Auclair, Guibert, Bender, & Weber, 2014; Smith et al.,
73 2017; Watanabe, Suetake, Tada, & Tajima, 2002), with the relative expression of *Dnmt3b* and
74 *Dnmt3a* being considerably reduced in the extraembryonic ectoderm (ExE) and trophoblast

75 lineages (Senner, Krueger, Oxley, Andrews, & Hemberger, 2012; Smith et al., 2017). This
76 discrepancy in *Dnmt3a* and *Dnmt3b* expression levels coincides with the initiation of divergent
77 DNA methylation acquisition between the trophoblast and the inner cell mass of the blastocyst
78 (Fulka, Mrazek, Tepla, & Fulka, 2004; Guo et al., 2014; Monk, 1987; Nakanishi et al., 2012; Oda,
79 Oxley, Dean, & Reik, 2013; Santos, Hendrich, Reik, & Dean, 2002; Smith et al., 2014), a
80 difference that becomes extremely apparent by E6.5, as the epiblast has acquired most of its global
81 DNA methylation compared to the lower-methylation state of the ExE (Auclair et al., 2014; Smith
82 et al., 2017; Zhang et al., 2018). This divergence is a common feature across mammalian placenta,
83 as a heterogeneous and lower-methylation state compared to somatic tissues and other cell types
84 is constantly observed (Chatterjee et al., 2016; Decato, Lopez-Tello, Sferruzzi-Perri, Smith, &
85 Dean, 2017; Schroeder et al., 2013; Smith et al., 2017).

86 Although the functional role of reduced methylation levels observed across the placental
87 genome is still not fully understood, studies suggest that it may activate transposable elements that
88 are typically silenced in other tissues (Chuong, 2013). DNA methylation plays an important role
89 in suppressing retrotransposons in mammalian cells, for which the activity has been associated
90 with genomic instability and disease development (Church et al., 2009; Slotkin & Martienssen,
91 2007). Following the *de novo* methylation wave, in embryonic-derived cells from the inner cell
92 mass, transposable elements acquire higher levels of DNA methylation causing transcriptional
93 silencing, whereas in the trophectoderm-derived cells that will form the placenta, these
94 transposable elements are maintained in a relaxed methylation state and preferentially expressed
95 (Okahara et al., 2004; Price et al., 2012; Warren et al., 2015). The low-methylation levels on these
96 elements contributed to the evolution and diversification of the placenta function through the
97 regulation of gene expression by providing placenta-specific enhancers, cryptic promoters and
98 other cis-regulatory elements (Cohen et al., 2011; Emera & Wagner, 2012; Haig, 2012; Macaulay,
99 Weeks, Andrews, & Morison, 2011; Mi et al., 2000; Xie et al., 2013).

100 Despite the evident distinction between embryonic and placental DNA methylation levels,
101 it remains unclear how, when and where methylation levels are acquired unequally across these
102 genomes. To better understand the developmental dynamics of epigenetic asymmetry that exists
103 between embryo and placenta, we first generated high-resolution maps of DNA methylation marks
104 using Reduced Representation Bisulfite Sequencing (RRBS) at mid-gestation, when the mouse
105 placenta is first considered mature (E10.5), to identify embryo-placenta differentially methylated

106 regions (DMRs). Then, using publicly available DNA methylation data sets and computational
107 analyses, we defined how various categories of DMRs are established in early stages and
108 maintained throughout development. In addition, we outlined the contribution of *Dnmt3a* and
109 *Dnmt3b* in the acquisition and maintenance of embryonic and extraembryonic specific DMR
110 patterns.
111
112 **METHODS**
113 ***Animals and Sample Collection***
114 Female C57BL/6N (8-10 week-old) were purchased from Harlan Sprague-Dawley
115 Laboratories (Indianapolis, IN) and were mated with male C57BL/6N (4 months of age).
116 Following natural mating, embryos and placental tissues were collected at E10.5 (presence of
117 vaginal plug at E0.5). Maternal decidua was removed from placentas. Samples were frozen
118 immediately in liquid nitrogen and stored at -80 °C until analyzed.
119
120 ***DNA Methylation Analyses***
121 RRBS libraries were generated as published protocols (Boyle et al., 2012; Gu et al., 2011)
122 with our specifications (Legault, Chan, & McGraw, 2019; Magnus et al., 2014; McGraw et al.,
123 2015). 500 ng of extracted DNA (Qiagen) from placenta (male n=2, female n=2) and embryo (male
124 n=2, female n=2) samples was *MspI* digested, adaptor ligated and PCR amplified (multiplex).
125 Multiplexed samples were pooled and 100 bp paired-end sequenced (HiSeq-2000, Illumina). The
126 data analyses were done according to the pipeline established at the McGill Epigenomics Mapping
127 and Data Coordinating Centers (Magnus et al., 2014; McGraw et al., 2015) that include BSMAP
128 and methylKit. Specific parameters were chosen including 100 bp step-wise tiling windows,
129 containing a minimum of 2 CpGs per tile and a minimum 15× CpG coverage of each tile per
130 sample. The methylation level of a 100-bp tile was the result of all CpG C/T read counts within
131 the tile after coverage normalization between samples, and the methylation level reported for a
132 sample on autosomal chromosomes was the average methylation level across all individual
133 replicates. Significant DNA methylation changes were designated as ±≥20% average differences
134 between groups of replicates and a q-value < 0.01 using the logistic regression function of
135 methylKit (Akalin et al., 2012). Direct comparisons between DNA methylation averages were
136 done using Wilcoxon-Mann-Whitney test in R. Gene ontology (GO) terms and pathway analyses

137 for RefSeqs associated to promoter-TSS were conducted using Metascape gene annotation and
138 analysis resource (Zhou et al., 2019).
139
140 ***Sequencing Data***
141 Publicly available DNA methylation data sets (Auclair et al., 2014; Decato et al., 2017;
142 Hon et al., 2013; Smith et al., 2014; Smith et al., 2017; Whidden et al., 2016) were analyzed using
143 a custom script to intersect single CpG site methylation calls from these data sets within defined
144 100bp tiles associated to the embryo-placenta DMRs categories
145
146 **RESULTS**
147 ***Increased Fluctuation in Genome-Wide DNA Methylation Levels in Placental Cells***
148 To identify the overall epigenetic asymmetry that exists between placental and embryonic
149 genomes during mouse *in utero* development, we first established genome-wide DNA methylation
150 profiles using RRBS (Legault et al., 2019; Magnus et al., 2014; McGraw et al., 2015) of embryos
151 and their corresponding placentas at mid-gestation (E10.5), the developmental stage at which the
152 mouse placenta is considered mature (Cross, Werb, & Fisher, 1994). Using this approach, we
153 quantified the DNA methylation profiles of ~1.8 million CpG sites in each sample (embryo n=4,
154 placenta n=4). We found that the accumulation of CpG methylation was very distinct between the
155 placenta and the embryo. In the placenta, we detected a greater proportion of CpGs in the 0-50%
156 methylation range and a lower proportion of CpGs in the 80-100% methylation range (Figure 1A).
157 Although we observed that a large proportion of CpGs within the examined regions had no
158 methylation marks in both the embryo and the placenta, interestingly, most CpGs with partial
159 methylation (20-50%) in placenta showed high methylation levels (>80%) in embryos (Figure 1B).
160 The divergence in global DNA methylation profiles conferred a high degree of clustering between
161 both tissue types (Figure S1). These results are consistent with previous studies indicating lower
162 levels of overall DNA methylation in extraembryonic tissues (Price et al., 2012; Schroeder et al.,
163 2013; Smith et al., 2017), reviewed in (Robinson & Price, 2015).
164 To further investigate the dynamics of DNA methylation between placental and embryonic
165 genomes and enable direct comparison of precise regions, we segmented the genome of autosomal
166 chromosomes into 100bp non-overlapping genomic windows (*tiles*; see methods section). After
167 removal of sex chromosomes, we identified 245 048 unique sequenced tiles (referred to as All-

168 tiles) containing 896 820 common CpGs between all placenta and embryo samples and with a
169 minimum of 15x sequencing depth. We observed a strong reduction in the fraction of highly
170 methylated tiles (80-100%) in the placenta compared to the embryo (Figure 1C), which correlated
171 with a sharp increase in the number of placenta tiles in the 0-20%, 20-40% and 40-60%
172 methylation range. Globally, we found that the average DNA methylation level across all placental
173 tiles was significantly lower compared to all embryo tiles (27% vs 45%, $p<0.0001$) (Figure 1C).
174 This overall epigenetic disparity in embryo and placenta DNA methylation levels was especially
175 noticeable when we mapped the methylation mean of All-tiles with respect to regions surrounding
176 the transcription start sites (TSS) (Figure 1D). When we focused on a specific chromosome section
177 (e.g., chr 7, 35Mb) (Figure 1E), we observed that genomic segments with high DNA methylation
178 levels in embryos had predominantly lower levels in placenta. We also observed that gene or CpG
179 island (CGI) poor regions had consistently high methylation levels in embryos and lower
180 methylation levels in the placenta. Together, these results indicate that the mid-gestation placenta
181 has very distinctive global DNA methylation levels compared to the embryo, and that this lower
182 level of global DNA methylation across the placental genome is due to a significant lower number
183 of highly methylated (≥80%) genomic regions. We can also conclude that despite the cellular
184 heterogeneity in E10.5 placental and embryonic tissues, the vast majority of the conceptus
185 possesses specific genomic regions with either low (0-20%) or high (80-100%) levels of
186 methylation. However, the placenta genome presents an increased number of regions having a
187 broader distribution of DNA methylation (20-80%), revealing a greater diversity in methylation
188 levels across placental cell types compared to embryonic cell types.
189
190 ***Embryonic and Placental DNA Methylation Divergences across Genomic Features***
191 To explain the developmentally divergent methylated states between the mouse embryo
192 and the placenta, we next sought to precisely determine the genomic features revealing DNA
193 methylation differences. We defined differentially methylated regions (DMRs) as 100bp genomic
194 segments showing a significant difference of methylation levels between embryonic and placental
195 samples with an absolute mean methylation difference of 20% or higher (McGraw et al., 2015;
196 Piche et al., 2019; Shaffer et al., 2015). Using these conditions, we screened the 245 048 unique
197 tiles common between all samples and identified 110 240 DMRs (~45% of All-tiles;
198 Supplementary Table 1) with tissue- and/or developmental-specific DNA methylation variations

199 between the embryo and the placenta (Figure2A; random subset of 20,000 DMRs shown).
200 Consistent with our findings (Figure 1), the majority (96.8%; n=106 712) of DMRs had lower
201 DNA methylation in the placenta (referred to as Hypo-DMRs) and only a small proportion (3.2%;
202 n=3 528) showed increased methylation levels (referred to as Hyper-DMRs) compared to the
203 embryo (Figure S2). For Hypo-DMRs, tiles mainly overlapped (96%; n=102 982) with intergenic,
204 intron, exon and promoter-TSS regions (Figure S2). For each of the genomic feature categories of
205 Hypo-DMRs, the average DNA methylation levels in the placenta were essentially half of those
206 present in the embryo (Figure 2B). As for DMRs with higher methylation levels in the placenta
207 (Hyper-DMRs), we noticed that the vast majority of these tiles (83%; n=2 929) had low
208 methylation levels in the embryo (<20%) (Figure 2A-B). Most of Hyper-DMRs overlapped
209 intergenic, intron, exon and promoter-TSS regions (93%; n=3 272, Figure S2). We then
210 investigated the relationship between gene expression and DMR DNA methylation levels. Highly
211 expressed genes in placental tissue such as *Syna* (*Syncytin A*) (Mi et al., 2000) showed overall
212 lower methylation levels in the placenta when compared to the embryo (Figure 2D, smoothed
213 representation) (Hansen, Langmead, & Irizarry, 2012). Similar observations were made in the gene
214 body of *Atf6b* (*Activating Transcription Factor 6 Beta*), a gene implicated in the transcriptional
215 downregulation of *Pgf* (*Placental Growth Factor*) in response to endoplasmic reticulum stress in
216 pathological placentas (Mizuuchi et al., 2016). As for genes predominantly expressed in the
217 embryo, *Mir219a-2/Mir219b*, a brain-specific non-coding microRNA, showed higher methylation
218 in the placenta (Figure 2D). It was recently shown that *Mir219* was abnormally expressed during
219 pregnancy in amnion retrieved specifically from obese women (Nardelli et al., 2014) and,
220 interestingly, obesity has been suggested to cause epigenetic changes (Lillycrop & Burdge, 2011).
221 Another example of placenta Hyper-DMRs is *Sox6* (*SRY-Box 6*), which is implicated in the
222 terminal differentiation of muscle (Figure 2D) (Kamachi & Kondoh, 2013). These observations
223 point to an association between tissue-specific DNA methylation levels of DMRs and biological
224 functions. Gene ontology enrichment analyses further support that promoter-associated Hypo-
225 DMRs were strongly associated to germline functions and reproduction (*e.g.*, male and female
226 gamete generation, reproduction, piRNA metabolic process, meiotic cell cycle, germ cell
227 development) (Figure 2C). As for promoter-associated Hyper-DMRs, top biological processes
228 were mostly associated with developmental and differentiation processes (*e.g.*, regionalization,
229 embryo development, pattern specification process, skeletal system, head development) (Figure

230 2C). Fittingly, the biological functions were completely divergent between Hypo- and Hyper-
231 DMRs. Altogether, these results denote that Hypo- and Hyper-DMRs are present across genomic
232 features between mid-gestation embryo and placenta, and that these DNA methylation divergences
233 are implicated in promoting/repressing specific processes during embryonic and placental
234 development.
235
236 ***Presence of Distinctive DMR Categories between Mid-Gestation Embryo and Placenta***
237 Amongst DMRs, our analyses also suggest the presence of particular DMR categories
238 based on their level of DNA methylation in the embryo and placenta (Figure 2A). By defining
239 subsets of DMRs and establishing their dynamic properties between tissues, we might better
240 understand the genome-wide asymmetry in DNA methylation levels observed between the embryo
241 and the placenta. To do so, we first clustered DMR-associated tiles in 6 different categories based
242 on their range of low, mid and high methylation level (Low; <20%, Mid; ≥20 to <80%, High;
243 ≥80%) in the embryo and the placenta, and followed the DMR category transitions between both
244 tissues. We observed that DMRs with High-levels of methylation in the embryo overlapped with
245 a large proportion of DMRs that showed Mid-levels of methylation in the placenta (Figure 3A,B;
246 High-Mid n=72 715), whereas only a fraction corresponded to DMRs with Low-levels of
247 methylation in the placenta (Figure 3A,B; High-Low n=1 889). As for DMRs with Mid-levels of
248 methylation in embryo, the largest part remained in that same Mid-levels category in the placenta
249 (Figure 3A; Mid-Mid n=23 640). Nonetheless, a portion of these embryonic Mid-levels DMRs
250 were directed to DMRs with either Low- (Figure 3A; Mid-Low n=9 055) or High- (Figure 3A;
251 Mid-High n= 21) levels of methylation in the placenta. Finally, DMRs with Low-levels of
252 methylation in the embryo all showed Mid-levels of methylation in the placenta (Figure 3A; Low-
253 Mid n=2 920). Thus, when we subdivide our DMRs into distinctive categories, we uncover that
254 embryonic cells possess a large proportion of DMRs of High-level (≥80%) of DNA methylation,
255 which remain potentially static in embryonic tissues, whereas the vast majority of these DMRs
256 have lower and wide-range DNA methylation levels within placental tissue.
257
258 ***Specific Genomic Features Associated with DMR Categories***
259 We next aimed to determine if the genomic distribution of embryo-placenta DMR
260 categories was associated with distinct genomic features. First, by classifying by genomic

261 annotations, we observed that DMRs with reduced methylation levels in the placenta (High-Mid,
262 High-Low, Mid-Low) were prevailingly found in intergenic regions (>50% of tiles) (Figure 3C),
263 whereas DMR categories with equivalent (Mid-Mid) or greater methylation level (Mid-High,
264 Low-Mid) in the placenta were more frequent in genic associated regions (>50% of tiles).
265 However, divergence between DMR categories was observed when we performed ontology
266 analyses on promoter regions (Figure S3), as each DMR subtype clearly showed distinct biological
267 functions. For example, High-Mid DMRs top functions were related to genes (e.g., *Aszl, Tnp1*,
268 *Piwil2*) associated with male gamete generation, piRNA metabolic process and male meiotic
269 nuclear division, whereas those of the Low-Mid category were mostly associated with
270 developmental aspects (e.g., skeletal system development, regionalization, nervous system
271 development). Since we know that in placenta, activation of retrotransposon-derived genes is
272 interrelated with low DNA methylation levels (Cohen et al., 2011; Macaulay et al., 2011; Reiss,
273 Zhang, & Mager, 2007), we next assessed how DMR categories overlapped with major types of
274 retrotransposons (LINE; long interspersed nuclear elements, SINE; short interspersed nuclear
275 element, and LTR; long terminal repeats). Out of the DMR categories, those with High-levels of
276 methylation in the embryo and either Mid- or Low-levels in the placenta (High-Mid and High-
277 Low) showed the most enriched overlap with retrotransposons, with 92% and 96% respectively
278 (Figure 3D). DMR categories associated with higher level of methylation in the placenta (Mid-
279 High and Low-Mid) showed the least overlap with retrotransposons, especially the Low-Mid
280 subtype. This highlights that during the *de novo* acquisition of DNA methylation patterns, DMRs
281 with High-levels of methylation in the embryo and lower levels in the placenta are almost
282 exclusively within retrotransposons-associated sequences, whereas DMRs with Low-levels of
283 methylation in the embryo and higher DNA methylation in the placenta are preferentially outside
284 retrotransposons-associated sequences. Finally, we investigated the proximity of the DMR
285 categories in regards to CpG rich (CpG islands; CGI), neighbouring (shore; < 2kb away from
286 CGIs, shelf; 2-4kb away from CGIs) and distant (open sea; > 4kb away from CGIs) regions (Figure
287 3E). We observed that most DMR categories are depleted from CGIs and are mostly found in open
288 sea regions. In contrast, ~60% of tiles in Low-Mid DMRs overlapped with CGI, shores and
289 shelves, revealing that the acquisition of *de novo* methylation for these genomic fragments in the
290 extraembryonic lineage preferentially targets sequences inside or surrounding CGIs.

291 Altogether, these results indicate that the asymmetry within DMR categories, based on their
292 methylation levels in the embryo and the placenta, can be associated to specific biological
293 functions and genomic-derived features (e.g., CpG, retrotransposon contents). This is particularly
294 apparent for DMRs with High-levels in the embryo (High-Mid, High-Low) and those with higher
295 methylation levels in the placenta (Low-Mid).
296
297 ***DMR Categories are Established During the De Novo Methylation Wave and Maintained***
298 ***Throughout Development***
299 To gain insights into the kinetics of lineage-specific DMR establishment between mid-
300 gestation embryo and placenta, as well as their status during development, we assessed the levels
301 of methylation associated with tiles for each DMR category as a function of their developmental
302 stage. Publicly available sequencing data (Smith et al., 2012; Whidden et al., 2016) were analyzed
303 using our custom script to generate 100bp tiles, and the DNA methylation levels for each tile were
304 calculated. In E3.5 blastocysts, when the mouse genome is mostly depleted from DNA methylation
305 marks, we observed low global DNA methylation levels (average <20%) for all DMR subtypes,
306 with similar median levels between the committed cells of the inner cell mass (ICM) and
307 trophectoderm lineages (Figure 4). DNA methylation levels tended to be higher in the
308 trophectoderm for regions falling in the Mid-High DMRs, although measurements are based on
309 very few DMRs for this specific category (n=21, Figure 3B, Mid-High). Since global DNA
310 methylation is re-acquired in the next few subsequent developmental stages, we then asked
311 whether the contrast in DNA methylation levels associated with the various DMR categories at
312 mid-gestation would already be present between E6.5 epiblast and extraembryonic ectoderm (ExE)
313 cell lineages, layers that are mostly composed of homogeneous and undifferentiated cell
314 populations. For all DMR categories, DNA methylation levels in the E6.5 epiblast and ExE already
315 showed similar pattern trends to those observed in the E10.5 embryo and placenta (Figure 4, Table
316 S2). Interestingly, for all DMR categories we observed slightly higher DNA methylation levels in
317 E6.5 ExE compared to E10.5 placenta (Figure 4, Table S2). However, when measured in the
318 subsequent developmental stages (E10.5, E11.5, E15 and E18), levels associated with each
319 category stabilized and remained in the same methylation range. This is true for all categories,
320 except for the Mid-High DMRs where methylation levels are reduced by ~20% at E18. As for the
321 E6.5 epiblast DNA methylation profiles, they closely matched those observed in the E10.5 embryo,

322 except again for the Mid-High DMRs. For each of the DMR subtypes, the DNA methylation levels
323 were largely stable and persisted across other time points (E6.5, E10.5, E11.5) in embryonic cells.
324 Although no public DNA methylation data were available for whole embryos at later stages, when
325 we overlapped tiles associated with E10.5 DMR categories with data from differentiated tissues of
326 adult mice, the global DNA methylation profiles closely matched those for the majority of DMR
327 categories (High-Mid, High-Low, Mid-Mid and Mid-Low) (Figure 4, Figure S4). We conclude
328 that the various DMR categories observed at E10.5 are established during the embryonic and
329 extraembryonic lineage-specification processes occurring during the peri-implantation wave of *de*
330 *novo* methylation, and that these DNA methylation landscapes are widely retained throughout
331 embryo and placenta development. Furthermore, for most DMR categories, the DNA methylation
332 levels observed in developing embryos are long-lasting and conserved throughout somatic cell
333 differentiation.
334
335 ***Dnmt3a- or Dnmt3b-Deficiency Alters Proper Establishment of DMR-Associated Patterns***
336 Since the combined activity of DNMT3A and DNMT3B is essential for proper
337 establishment of DNA methylation profiles and normal development, we next sought to define the
338 contribution of each enzyme in the *de novo* establishment of DNA methylation in subtypes of
339 DMRs in embryonic and extraembryonic cell lineages. To do so, we used DNA methylation data
340 from publicly available datasets (whole genome bisulfite sequencing and RRBS) at E6.5 (epiblast
341 and ExE) (Smith et al., 2017) and E8.5 (embryo) (Auclair et al., 2014) with various inactive forms
342 of *Dnmts*. First, when we overlapped our All-tiles subset, we observed a substantial reduction
343 ($p<0.0001$) in average DNA methylation in absence of DNMT3A (37.81%) or DNMT3B (31.48%)
344 in the E6.5 epiblast compared to wild-type (44.81%), whereas in the E6.5 ExE such a comparable
345 loss was only associated with a *Dnmt3b*-deficiency (wt: 34.38% vs *Dnmt3b*$^{-/-}$: 19.33%, $p<0.0001$)
346 (Figure S5). Similarly, in the E8.5 embryo, a significant reduction in average DNA methylation
347 level was measured with lack of *Dnmt3a* or *Dnmt3b* expression compared to wild-type (wt: 47.5%;
348 *Dnmt3a*$^{-/-}$: 43.6%; *Dnmt3b*$^{-/-}$: 34%, $p<0.0001$) (Figure S5). For most DMR subtypes, absence of
349 DNMT3A caused modest or no reduction on overall DNA methylation levels in E6.5 epiblast and
350 ExE (Figure 5A, Table S3). Intriguingly, *Dnmt3a*-deficiency caused a slight gain of methylation
351 (wt: 76.9% vs *Dnmt3a*$^{-/-}$: 81.5%, $p<0.0001$) level in the E6.5 epiblast for High-Mid DMRs,
352 suggesting a potential overcompensation effect by DNMT3B in the epiblast on this specific DMR

353 subtype. In comparison, *Dnmt3b*-depletion led to a substantial loss of average methylation levels
354 in all DMR categories in the E6.5 epiblast and ExE, except for epiblast High-Mid DMRs (Figure
355 5A, Table S3) for which a compensatory mechanism provided high levels of methylation (wt:
356 76.9% vs *Dnmt3b*$^{-/-}$: 71.6%). The compensatory mechanism on High-Mid DMRs in response to
357 *Dnmt3b*-deficiency was ineffective in the E6.5 ExE. When we focused on promoter-TSS for each
358 DMR categories, we observed again that loss of methylation for these regulatory regions was
359 principally associated with *Dnmt3b*-deficiency (Figure 5B). The promoter-TSS regions associated
360 with High-Mid DMRs retained relatively high methylation levels for either *Dnmt3a*$^{-/-}$ or *Dnmt3b*$^{-}$
361 $^{/-}$ epiblast samples, demonstrating a robust and compensatory *de novo* methylation mechanism. To
362 further underline the impact of DNMT3A or DNMT3B on the *de novo* methylation of DMRs, we
363 measured methylation levels for DMRs selected from our gene enrichment analyses (*Fgb*, *P2rx7*,
364 *Pcyt2*, *Etnppl*, *Ralgds*, *Lrp5*) and other genomic segments covered by multiple tiles (*Cxxc1*, *Fcgrt*,
365 *Lamp5*, *Mbd1*, *Lphn1*, *Pick1*, *Irf1*) (Figure S6 & S7) in *Dnmt3a*- or *Dnmt3b*-deficient epiblast and
366 ExE. In line with our global observations, for most DMR-associated tiles, a *Dnmt3b*-deficiency in
367 E6.5 epiblast or ExE caused a more severe loss of methylation compared to lack of *Dnmt3a.*
368 However, for some regions in the E6.5 epiblast (e.g., *Pick1*, *Irf1*), *Dnmt3a*$^{-/-}$ methylation levels
369 were lower to those of *Dnmt3b*$^{-/-}$. Overall, we show that of DNMT3A and DNMT3B participate
370 in the establishment of the asymmetric methylation patterns associated with the various DMR
371 categories in both embryonic and extraembryonic cells, with DNMT3B being the principal
372 contributor in both cell lineages during the *de novo* reprogramming wave as it can compensate
373 almost entirely for the absence of DNMT3A.
374
375 ***Decline in Compensatory DNA Methylation Mechanisms in Response to Dnmt3a- or Dnmt3b-***
376 ***Deficiency.***
377 As embryonic development progresses from E6.5 to E8.5, our data suggest that lack of
378 DNMT3A or DNMT3B further reduces global methylation levels of DMRs (High-Mid, High-
379 Low, Mid-Low and Mid-Mid), evoking that absence of either enzymatic activity causes an additive
380 and extended effect (Figure 5A-B). To further define the robustness in compensatory mechanism
381 between DNMT3A or DNMT3B in the establishment and maintenance of DNA methylation on
382 DMRs categories, we focused on High-Mid promoter-TSS- associated DMRs as they have the
383 highest DNA methylation levels and require the most *de novo* methyltransferase activity.

384 Methylation differences of ≥20% between wild-type and *Dnmt3a*- or *Dnmt3b*-deficient samples
385 were considered as regions showing substantial lack of compensation. In agreement with our
386 results (Figure 5A-B), we observed that at E6.5, DNMT3B can compensate almost entirely for
387 DNMT3A loss by maintaining methylation levels on most promoters-TSS associated tiles in the
388 epiblast (410/437 = 93.8%) and ExE (558/602 = 92.7%), whereas DNMT3A can only partially
389 alleviate the lack of DNMT3B in the epiblast (315/410 = 78.6%) and ExE (244/524 = 46.6%)
390 (Figure 6A-B). As embryonic cell lineages development evolves between E6.5 and E8.5, global
391 methylation levels increase on promoter-TSS of High-Mid DMRs. However, we detected a sharp
392 decline in the compensatory mechanism to rescue the *de novo* and/or maintenance of methylation
393 levels of promoter-TSS DMRs in the *Dnmt3a*- (524/627 = 80.9%) or *Dnmt3b*- (256/622 = 41.2%)
394 deficient E8.5 embryos. This is further highlighted when we focus on a subgroup of 314 promoter-
395 TSS associated tiles overlapping all of 9 data sets (Figure 6C), including gene promoters (e.g.,
396 *Asz1, Catsper1, Ccdc42, Dmrtb1, Piwil2, Rpl10l, Sox30, Sycp1, Tnp1, Ttll1, Zfn42*) related to our
397 top enriched biological functions (i.e., piRNA, gamete generation and germ cells, meiotic nuclear
398 division). Although E8.5 *Dnmt3a*- or *Dnmt3b*-deficient ExE data was not available, our data
399 suggest that greater compensation failure would also be observed in this tissue. Thus, embryonic-
400 placental DMRs need the combined action of DNMT3Aand DNMT3Bto both establish and
401 maintain proper asymmetric levels during early development as compensatory DNA methylation
402 mechanisms during the *de novo* wave of methylation decline overtime and fail to overcome
403 methyltransferase shortage in later development stages.
404
405 **DISCUSSION**
406 With recent breakthroughs in high-throughput sequencing, we now have a better
407 understanding of the dynamic of DNA methylation erasure occurring in early cleavage stage
408 embryos following fertilization. However, the discrepancies in acquisition of genome-wide DNA
409 methylation patterns in early post-implantation embryonic and extraembryonic cell lineages
410 remain to be methodically delineated. To address this issue and further our understanding of the
411 DNA methylation asymmetry that guides the developmental trajectory of embryonic and
412 extraembryonic cell lineages, we established genome-wide DNA methylation profiles of mouse
413 embryo and placenta at mid-gestation, and analyzed various publicly available developmental
414 stage specific embryo and placenta DNA methylation datasets. Using this strategy, we uncovered

415 that 45% of the genomic regions analyzed differ in DNA methylation status (≥20%) between mid-
416 gestation embryo and placenta, and that these DMRs can be further divided into categories based
417 on their levels of DNA methylation (Low; <20%, Mid; ≥20 to <80%, High; ≥80%) in the embryo
418 and placenta. We show that the embryo and placenta acquire specific DMR categories during the
419 early stage of the *de novo* DNA methylation wave, and that these DMRs persist throughout prenatal
420 development, as well as into somatic adult tissues. Furthermore, we show that *Dnmt3b* primarily
421 drives the divergence in DNA methylation levels associated with these specific DMRs and that *de*
422 *novo* methyltransferase activity of *Dnmt3b* can almost entirely compensate for lack of *Dnmt3a* in
423 the asymmetric establishment of embryonic and placental DMRs, but that *Dnmt3a* can only
424 partially compensate the absence of *Dnmt3b*. However, with developmental progression, this
425 compensatory DNA methylation mechanism becomes less effective.

426 Our results indicate that the kinetics of DNA methylation acquisition leading to specific
427 embryo-placenta DMR categories is not a stepwise process occurring throughout cell fate
428 decisions and patterning of embryonic and extraembryonic lineages, but a prompt progression in
429 the early post-implanted conceptus. These results are in line with studies reflecting that the
430 initiation of asymmetric DNA methylation levels begins within the trophoblast and the inner cell
431 mass of the blastocyst (Santos et al., 2002), and becomes highly evident by the time the epiblast
432 acquires its initial global DNA methylation patterns at E6.5 during the *de novo* reprogramming
433 wave (Auclair et al. 2014, Smith et al. 2017). Our results show that the acquisition period between
434 E4.5 and E6.5 is particularly key to establishing asymmetric DNA methylation patterns associated
435 with mid-gestation embryo-placenta DMR classes, and that these DMR associated-patterns are
436 long-lasting across stages of prenatal development. Since we studied cell populations derived from
437 embryonic and placental tissues, we cannot dismiss the prevalence of cell-to-cell heterogeneity in
438 the acquisition kinetics of specific DMR patterns. Despite this concern, our results indicate that
439 embryonic cells have a large body of DMRs with High-levels (≥80%) and Low-levels (<20%) of
440 methylation that remain static across development, as well as in somatic cell types (High-Mid &
441 High-Low DMRs), whereas compared to the embryo, the placental DMRs have overall lower
442 methylation levels and are more broadly distributed amongst methylation levels, which has also
443 been shown in other studies where genome-wide DNA methylation profiles of placental cells were
444 compared to other tissues and specific cell types (Schroeder et al., 2013; Chatterjee et al., 2016;
445 Smith et al., 2017). Lower methylation levels in the placenta have been associated with reduced

446 *de novo* methyltransferase activity in the ExE during the *de novo* reprogramming wave (Fulka et
447 al., 2004; Santos et al., 2002). Nevertheless, we observe methylation level peaks for all DMR
448 categories within the ExE at E6.5 before levels stabilize at E10.5. As of now, the implication of
449 these methylation level peaks on future regulation mechanisms and methylation profiles is
450 unknown. Moreover, it remains to be determined whether global reduction in DNA methylation
451 marks on DMRs between the E6.5 and E10.5 extraembryonic cell lineages is stochastic or targeted,
452 and whether it occurs through passive or active mechanisms.

453 We also observed an enrichment of retrotransposons (i.e., LINE, SINE, LTR) in DMRs
454 especially in those with High-levels of methylation in the embryo and lower-levels in the placenta,
455 whereas DMRs with Low-levels of methylation in the embryo and higher levels in the placenta
456 are preferentially outside retrotransposons-associated sequences. Earlier findings of Chapman et
457 *al*. (Chapman, Forrester, Sanford, Hastie, & Rossant, 1984) revealed that repeat regions in the
458 placenta appear to lack tight control of their methylation patterns, perhaps indicating that
459 maintaining methylation, and therefore repression of these elements for genome stability and
460 integrity, is not critical given the relatively short lifespan of this organ. However, we do observe
461 Mid-range methylation levels (20-80%) in the placenta for a substantial portion of DMRs that are
462 associated with retrotransposons, revealing that specific genomic regions associated with
463 repetitive elements do need tight regulation in extraembryonic cell lineages for proper
464 development. These results are in line with findings exposing that the deletion of genome-defense
465 gene *Tex19.1* leads to the de-repression of LINE1 and compromises placental development,
466 suggesting that disparities between retrotransposon suppression and genome-defense mechanisms
467 might contribute to placenta dysfunction and disease (Reichmann et al., 2013).

468 DNMT3A and DNMT3B are required to establish proper methylation profiles on the
469 embryonic genome during the *de novo* reprogramming wave, as both methyltransferase enzymes
470 have redundant, but also specific functions. However, the activity of DNMT3B is the main
471 contributor in the acquisition of profiles in epiblast cells, and especially commands methylation
472 on CGIs associated with developmental genes (Auclair et al., 2014). Auclair et *al*. highlighted that
473 in the absence of DNMT3B, DNMT3A was not able to counterbalance, leading to the loss of
474 promoter-CGI methylation and gain of expression of germline genes (e.g., *Sycp1*, *Sycp2*, *Mael*,
475 *Rpl10l*, *Dmrtb1*) in somatic cells of the embryo. Here, we show that the promoter of these germline
476 genes, associated with meiotic and piRNA processes as well as other genes with similar biological

477 functions, are highly enriched in High-Mid DMRs. We also reveal that for this particular set of
478 High-Mid DMRs, mainly deprived of CGIs, DNMT3A is able to substantially counterbalance the
479 lack of DNMT3B in the E6.5 epiblast and establish global DNA methylation levels, whereas in
480 the ExE, this compensatory mechanism is rather inefficient. Globally, we show that DNMT3B is
481 much more potent at compensating than DNMT3A in both the epiblast and ExE for all DMR
482 categories, indicating that DNMT3B is the main *de novo* enzyme driving asymmetric DNA
483 methylation patterns between the embryo and placenta. Although compensatory mechanisms have
484 been observed in *Dnmt3a* or *Dnmt3b*-depleted conceptuses, we still do not fully understand the
485 process as *Dnmt3a* and *Dnmt3b* have cell lineage specific expression during the peri-implantation
486 developmental period. As development progresses, we observed that the compensation mechanism
487 in *Dnmt3a* or *Dnmt3b*-deficient embryos remains apparent at E8.5 on most DMR categories, but
488 is less effective as the methylation gaps increase compared to wild-type. This correlates with a
489 developmental period where DNMT3A is now the main *de novo* methyltransferase enzyme in both
490 the embryo and placenta (Okano et al., 1999; Watanabe et al., 2002), and with a compensatory
491 activity of DNMT3A being less effective. This suggests that DNMT3B activity is critical to ensure
492 proper establishment of DNA methylation asymmetry between the embryonic and extraembryonic
493 cell lineages during the *de novo* reprogramming wave, but that DNMT3A is required during the
494 developmental progression to safeguard methylation levels on DMR categories.
495
496 **CONCLUSION**
497 We demonstrate that asymmetry between embryo and placenta DNA methylation patterns
498 occurs rapidly during *de novo* acquisition of methylation marks in the early post-implanted
499 conceptus, and that these patterns are long-lasting across subtypes of DMRs. We also reveal that
500 at the peri-implantation stages, *de novo* methyltransferase activity of DNMT3B is the main
501 provider of asymmetric methylation marks on DMRs, and that it largely compensates the lack of
502 DNMT3A in the epiblast and ExE. However, as development progresses, DNMT3A becomes the
503 principal *de novo* methyltransferase by mid-gestation, and DNMT3B methyltransferase activity is
504 less effective at promoting compensation. These results further underline why embryos developing
505 without DNMT3B have severe DNA methylation defects and die at mid-gestation, whereas those
506 without DNMT3A only die postnatally. Further investigation is required to determine the
507 molecular mechanisms controlling the precise *de novo* acquisition of long-lasting methylation

508 marks on specific DMR subtypes in the embryonic and extraembryonic cell lineages, and how
509 errors in this process could lead to abnormal development and diseases.
510
511

512 **ACKNOWLEDGMENTS**

513 We thank the McGraw lab for critical comments and suggestions, as well as Elizabeth Maurice-
514 Elder for editing.

515

516 **COMPETING INTERESTS**

517 No competing interests declared

518

519 **FUNDING**

520 This work was supported by a research grant from the Natural Sciences and Engineering Research
521 Council of Canada. We acknowledge the Fonds de Recherche du Québec en Santé (S.M, L.M.L)
522 and the Réseau Québécois en Reproduction and Fonds de recherche du Québec – Nature et
523 technologies (K.D) for salary awards.

524

525 **DATA AVAILABILITY**

526 The data from this study have been submitted to the Gene Expression Omnibus (#GSE95610).
527 Reviewer link:
528 https://www.ncbi.nlm.nih.gov/geo/query/acc.cgi?token=ghsnmqoctlgjlcj&acc=GSE95610
529

530 **Table S1. Annotation and DNA methylation values associated with DMRs.**

531 **Table S2. DNA methylation levels for DMR categorises across development.**

532 **Table S3. DNA methylation levels for DMR categories in various *Dnmt* knockout mouse**
533 **models.**

534 **Table S4. Number of 100bp tiles in each category of public data that overlap with Embryo-**
535 **Placenta DMRs (related to Figure 4; 5A; S4; S5)**

536 **REFERENCES**

537 Akalin, A., Kormaksson, M., Li, S., Garrett-Bakelman, F. E., Figueroa, M. E., Melnick, A., &
538 Mason, C. E. (2012). methylKit: a comprehensive R package for the analysis of genome-wide
539 DNA methylation profiles. *Genome Biol, 13*(10), R87. doi:10.1186/gb-2012-13-10-r87
540 Auclair, G., Guibert, S., Bender, A., & Weber, M. (2014). Ontogeny of CpG island methylation
541 and specificity of DNMT3 methyltransferases during embryonic development in the mouse.
542 *Genome Biol, 15*(12), 545. doi:10.1186/s13059-014-0545-5
543 Bestor, T. H. (2000). The DNA methyltransferases of mammals. *Hum Mol Genet, 9*(16), 2395-
544 2402.
545 Boyle, P., Clement, K., Gu, H., Smith, Z. D., Ziller, M., Fostel, J. L., . . . Meissner, A. (2012). Gel-
546 free multiplexed reduced representation bisulfite sequencing for large-scale DNA methylation
547 profiling. *Genome Biol, 13*(10), R92. doi:10.1186/gb-2012-13-10-r92
548 Chapman, V., Forrester, L., Sanford, J., Hastie, N., & Rossant, J. (1984). Cell lineage-specific
549 undermethylation of mouse repetitive DNA. *Nature, 307*(5948), 284-286.
550 Chatterjee, A., Macaulay, E. C., Rodger, E. J., Stockwell, P. A., Parry, M. F., Roberts, H. E., . . .
551 Morison, I. M. (2016). Placental Hypomethylation Is More Pronounced in Genomic Loci
552 Devoid of Retroelements. *G3 (Bethesda), 6*(7), 1911-1921. doi:10.1534/g3.116.030379
553 Chuong, E. B. (2013). Retroviruses facilitate the rapid evolution of the mammalian placenta.
554 *Bioessays, 35*(10), 853-861. doi:10.1002/bies.201300059
555 Church, D. M., Goodstadt, L., Hillier, L. W., Zody, M. C., Goldstein, S., She, X., . . . Mouse
556 Genome Sequencing, C. (2009). Lineage-specific biology revealed by a finished genome
557 assembly of the mouse. *PLoS Biol, 7*(5), e1000112. doi:10.1371/journal.pbio.1000112
558 Cohen, C. J., Rebollo, R., Babovic, S., Dai, E. L., Robinson, W. P., & Mager, D. L. (2011).
559 Placenta-specific expression of the interleukin-2 (IL-2) receptor beta subunit from an
560 endogenous retroviral promoter. *J Biol Chem, 286*(41), 35543-35552.
561 doi:10.1074/jbc.M111.227637
562 Cross, J. C. (2000). Genetic insights into trophoblast differentiation and placental morphogenesis.
563 *Semin Cell Dev Biol, 11*(2), 105-113. doi:10.1006/scdb.2000.0156
564 Cross, J. C., Werb, Z., & Fisher, S. J. (1994). Implantation and the placenta: key pieces of the
565 development puzzle. *Science, 266*(5190), 1508-1518. doi:10.1126/science.7985020
566 Decato, B. E., Lopez-Tello, J., Sferruzzi-Perri, A. N., Smith, A. D., & Dean, M. D. (2017). DNA
567 Methylation Divergence and Tissue Specialization in the Developing Mouse Placenta. *Mol Biol*
568 *Evol, 34*(7), 1702-1712. doi:10.1093/molbev/msx112
569 Emera, D., & Wagner, G. P. (2012). Transposable element recruitments in the mammalian
570 placenta: impacts and mechanisms. *Brief Funct Genomics, 11*(4), 267-276.
571 doi:10.1093/bfgp/els013
572 Fulka, H., Mrazek, M., Tepla, O., & Fulka, J., Jr. (2004). DNA methylation pattern in human
573 zygotes and developing embryos. *Reproduction, 128*(6), 703-708. doi:10.1530/rep.1.00217
574 Gu, H., Smith, Z. D., Bock, C., Boyle, P., Gnirke, A., & Meissner, A. (2011). Preparation of
575 reduced representation bisulfite sequencing libraries for genome-scale DNA methylation
576 profiling. *Nat Protoc, 6*(4), 468-481. doi:10.1038/nprot.2010.190
577 Guo, H., Zhu, P., Yan, L., Li, R., Hu, B., Lian, Y., . . . Qiao, J. (2014). The DNA methylation
578 landscape of human early embryos. *Nature, 511*(7511), 606-610. doi:10.1038/nature13544
579 Haig, D. (2012). Retroviruses and the placenta. *Curr Biol, 22*(15), R609-613.
580 doi:10.1016/j.cub.2012.06.002

581 Hansen, K. D., Langmead, B., & Irizarry, R. A. (2012). BSmooth: from whole genome bisulfite
582 sequencing reads to differentially methylated regions. *Genome Biol, 13*(10), R83.
583 doi:10.1186/gb-2012-13-10-r83
584 Hirasawa, R., Chiba, H., Kaneda, M., Tajima, S., Li, E., Jaenisch, R., & Sasaki, H. (2008).
585 Maternal and zygotic Dnmt1 are necessary and sufficient for the maintenance of DNA
586 methylation imprints during preimplantation development. *Genes Dev, 22*(12), 1607-1616.
587 doi:10.1101/gad.1667008
588 Hon, G. C., Rajagopal, N., Shen, Y., McCleary, D. F., Yue, F., Dang, M. D., & Ren, B. (2013).
589 Epigenetic memory at embryonic enhancers identified in DNA methylation maps from adult
590 mouse tissues. *Nat Genet, 45*(10), 1198-1206. doi:10.1038/ng.2746
591 Howell, C. Y., Bestor, T. H., Ding, F., Latham, K. E., Mertineit, C., Trasler, J. M., & Chaillet, J.
592 R. (2001). Genomic imprinting disrupted by a maternal effect mutation in the Dnmt1 gene. *Cell,*
593 *104*(6), 829-838.
594 Kamachi, Y., & Kondoh, H. (2013). Sox proteins: regulators of cell fate specification and
595 differentiation. *Development, 140*(20), 4129-4144. doi:10.1242/dev.091793
596 Kaneda, M., Okano, M., Hata, K., Sado, T., Tsujimoto, N., Li, E., & Sasaki, H. (2004). Essential
597 role for de novo DNA methyltransferase Dnmt3a in paternal and maternal imprinting. *Nature,*
598 *429*(6994), 900-903. doi:10.1038/nature02633
599 Kato, Y., Kaneda, M., Hata, K., Kumaki, K., Hisano, M., Kohara, Y., . . . Sasaki, H. (2007). Role
600 of the Dnmt3 family in de novo methylation of imprinted and repetitive sequences during male
601 germ cell development in the mouse. *Hum Mol Genet, 16*(19), 2272-2280.
602 doi:10.1093/hmg/ddm179
603 Legault, L.-M., Chan, D., & McGraw, S. (2019). Rapid Multiplexed Reduced Representation
604 Bisulfite Sequencing Library Prep (rRRBS). *BIO-PROTOCOL, 9*(4).
605 Lei, H., Oh, S. P., Okano, M., Juttermann, R., Goss, K. A., Jaenisch, R., & Li, E. (1996). De novo
606 DNA cytosine methyltransferase activities in mouse embryonic stem cells. *Development,*
607 *122*(10), 3195-3205.
608 Leonhardt, H., Page, A. W., Weier, H. U., & Bestor, T. H. (1992). A targeting sequence directs
609 DNA methyltransferase to sites of DNA replication in mammalian nuclei. *Cell, 71*(5), 865-873.
610 doi:10.1016/0092-8674(92)90561-p
611 Li, E. (2002). Chromatin modification and epigenetic reprogramming in mammalian development.
612 *Nat Rev Genet, 3*(9), 662-673. doi:10.1038/nrg887
613 Li, E., Bestor, T. H., & Jaenisch, R. (1992). Targeted mutation of the DNA methyltransferase gene
614 results in embryonic lethality. *Cell, 69*(6), 915-926.
615 Lillycrop, K. A., & Burdge, G. C. (2011). Epigenetic changes in early life and future risk of
616 obesity. *Int J Obes (Lond), 35*(1), 72-83. doi:10.1038/ijo.2010.122
617 Macaulay, E. C., Weeks, R. J., Andrews, S., & Morison, I. M. (2011). Hypomethylation of
618 functional retrotransposon-derived genes in the human placenta. *Mamm Genome, 22*(11-12),
619 722-735. doi:10.1007/s00335-011-9355-1
620 Magnus, N., Garnier, D., Meehan, B., McGraw, S., Lee, T. H., Caron, M., . . . Rak, J. (2014).
621 Tissue factor expression provokes escape from tumor dormancy and leads to genomic
622 alterations. *Proc Natl Acad Sci U S A, 111*(9), 3544-3549. doi:10.1073/pnas.1314118111
623 McGraw, S., Zhang, J. X., Farag, M., Chan, D., Caron, M., Konermann, C., . . . Trasler, J. M.
624 (2015). Transient DNMT1 suppression reveals hidden heritable marks in the genome. *Nucleic*
625 *Acids Res*. doi:10.1093/nar/gku1386

Mi, S., Lee, X., Li, X., Veldman, G. M., Finnerty, H., Racie, L., . . . McCoy, J. M. (2000). Syncytin is a captive retroviral envelope protein involved in human placental morphogenesis. *Nature, 403*(6771), 785-789. doi:10.1038/35001608

Mizuuchi, M., Cindrova-Davies, T., Olovsson, M., Charnock-Jones, D. S., Burton, G. J., & Yung, H. W. (2016). Placental endoplasmic reticulum stress negatively regulates transcription of placental growth factor via ATF4 and ATF6beta: implications for the pathophysiology of human pregnancy complications. *J Pathol, 238*(4), 550-561. doi:10.1002/path.4678

Monk, M. (1987). Genomic imprinting. Memories of mother and father. *Nature, 328*(6127), 203-204. doi:10.1038/328203a0

Morgan, H. D., Santos, F., Green, K., Dean, W., & Reik, W. (2005). Epigenetic reprogramming in mammals. *Hum Mol Genet, 14 Spec No 1*, R47-58. doi:10.1093/hmg/ddi114

Nakanishi, M. O., Hayakawa, K., Nakabayashi, K., Hata, K., Shiota, K., & Tanaka, S. (2012). Trophoblast-specific DNA methylation occurs after the segregation of the trophectoderm and inner cell mass in the mouse periimplantation embryo. *Epigenetics, 7*(2), 173-182. doi:10.4161/epi.7.2.18962

Nardelli, C., Iaffaldano, L., Ferrigno, M., Labruna, G., Maruotti, G. M., Quaglia, F., . . . Sacchetti, L. (2014). Characterization and predicted role of the microRNA expression profile in amnion from obese pregnant women. *Int J Obes (Lond), 38*(3), 466-469. doi:10.1038/ijo.2013.121

Oda, M., Oxley, D., Dean, W., & Reik, W. (2013). Regulation of lineage specific DNA hypomethylation in mouse trophectoderm. *PLoS One, 8*(6), e68846. doi:10.1371/journal.pone.0068846

Okahara, G., Matsubara, S., Oda, T., Sugimoto, J., Jinno, Y., & Kanaya, F. (2004). Expression analyses of human endogenous retroviruses (HERVs): tissue-specific and developmental stage-dependent expression of HERVs. *Genomics, 84*(6), 982-990. doi:10.1016/j.ygeno.2004.09.004

Okano, M., Bell, D. W., Haber, D. A., & Li, E. (1999). DNA methyltransferases Dnmt3a and Dnmt3b are essential for de novo methylation and mammalian development. *Cell, 99*(3), 247-257.

Piche, J., Gosset, N., Legault, L. M., Pacis, A., Oneglia, A., Caron, M., . . . Andelfinger, G. (2019). Molecular Signature of CAID Syndrome: Noncanonical Roles of SGO1 in Regulation of TGF-beta Signaling and Epigenomics. *Cell Mol Gastroenterol Hepatol, 7*(2), 411-431. doi:10.1016/j.jcmgh.2018.10.011

Price, E. M., Cotton, A. M., Penaherrera, M. S., McFadden, D. E., Kobor, M. S., & Robinson, W. (2012). Different measures of "genome-wide" DNA methylation exhibit unique properties in placental and somatic tissues. *Epigenetics, 7*(6), 652-663. doi:10.4161/epi.20221

Reichmann, J., Reddington, J. P., Best, D., Read, D., Ollinger, R., Meehan, R. R., & Adams, I. R. (2013). The genome-defence gene Tex19.1 suppresses LINE-1 retrotransposons in the placenta and prevents intra-uterine growth retardation in mice. *Hum Mol Genet, 22*(9), 1791-1806. doi:10.1093/hmg/ddt029

Reiss, D., Zhang, Y., & Mager, D. L. (2007). Widely variable endogenous retroviral methylation levels in human placenta. *Nucleic Acids Res, 35*(14), 4743-4754. doi:10.1093/nar/gkm455

Robinson, W. P., & Price, E. M. (2015). The human placental methylome. *Cold Spring Harb Perspect Med, 5*(5), a023044. doi:10.1101/cshperspect.a023044

Rossant, J., & Cross, J. C. (2001). Placental development: lessons from mouse mutants. *Nat Rev Genet, 2*(7), 538-548. doi:10.1038/35080570

670 Santos, F., Hendrich, B., Reik, W., & Dean, W. (2002). Dynamic reprogramming of DNA
671 methylation in the early mouse embryo. *Dev Biol, 241*(1), 172-182.
672 doi:10.1006/dbio.2001.0501
673 Schroeder, D. I., Blair, J. D., Lott, P., Yu, H. O., Hong, D., Crary, F., . . . LaSalle, J. M. (2013).
674 The human placenta methylome. *Proc Natl Acad Sci U S A, 110*(15), 6037-6042.
675 doi:10.1073/pnas.1215145110
676 Senner, C. E., Krueger, F., Oxley, D., Andrews, S., & Hemberger, M. (2012). DNA methylation
677 profiles define stem cell identity and reveal a tight embryonic-extraembryonic lineage
678 boundary. *Stem Cells, 30*(12), 2732-2745. doi:10.1002/stem.1249
679 Shaffer, B., McGraw, S., Xiao, S. C., Chan, D., Trasler, J., & Chaillet, J. R. (2015). The dnmt1
680 intrinsically disordered domain regulates genomic methylation during development. *Genetics,*
681 *199*(2), 533-541. doi:10.1534/genetics.114.173609
682 Slotkin, R. K., & Martienssen, R. (2007). Transposable elements and the epigenetic regulation of
683 the genome. *Nat Rev Genet, 8*(4), 272-285. doi:10.1038/nrg2072
684 Smith, Z. D., Chan, M. M., Humm, K. C., Karnik, R., Mekhoubad, S., Regev, A., . . . Meissner,
685 A. (2014). DNA methylation dynamics of the human preimplantation embryo. *Nature,*
686 *511*(7511), 611-615. doi:10.1038/nature13581
687 Smith, Z. D., Chan, M. M., Mikkelsen, T. S., Gu, H., Gnirke, A., Regev, A., & Meissner, A. (2012).
688 A unique regulatory phase of DNA methylation in the early mammalian embryo. *Nature,*
689 *484*(7394), 339-344. doi:10.1038/nature10960
690 Smith, Z. D., Shi, J., Gu, H., Donaghey, J., Clement, K., Cacchiarelli, D., . . . Meissner, A. (2017).
691 Epigenetic restriction of extraembryonic lineages mirrors the somatic transition to cancer.
692 *Nature, 549*(7673), 543-547. doi:10.1038/nature23891
693 Warren, I. A., Naville, M., Chalopin, D., Levin, P., Berger, C. S., Galiana, D., & Volff, J. N.
694 (2015). Evolutionary impact of transposable elements on genomic diversity and lineage-
695 specific innovation in vertebrates. *Chromosome Res, 23*(3), 505-531. doi:10.1007/s10577-015-
696 9493-5
697 Watanabe, D., Suetake, I., Tada, T., & Tajima, S. (2002). Stage- and cell-specific expression of
698 Dnmt3a and Dnmt3b during embryogenesis. *Mech Dev, 118*(1-2), 187-190.
699 Whidden, L., Martel, J., Rahimi, S., Richard Chaillet, J., Chan, D., & Trasler, J. M. (2016).
700 Compromised oocyte quality and assisted reproduction contribute to sex-specific effects on
701 offspring outcomes and epigenetic patterning. *Hum Mol Genet*. doi:10.1093/hmg/ddw293
702 Xie, M., Hong, C., Zhang, B., Lowdon, R. F., Xing, X., Li, D., . . . Wang, T. (2013). DNA
703 hypomethylation within specific transposable element families associates with tissue-specific
704 enhancer landscape. *Nat Genet, 45*(7), 836-841. doi:10.1038/ng.2649
705 Zhang, Y., Xiang, Y., Yin, Q., Du, Z., Peng, X., Wang, Q., . . . Xie, W. (2018). Dynamic
706 epigenomic landscapes during early lineage specification in mouse embryos. *Nat Genet, 50*(1),
707 96-105. doi:10.1038/s41588-017-0003-x
708 Zhou, Y., Zhou, B., Pache, L., Chang, M., Khodabakhshi, A. H., Tanaseichuk, O., . . . Chanda, S.
709 K. (2019). Metascape provides a biologist-oriented resource for the analysis of systems-level
710 datasets. *Nat Commun, 10*(1), 1523. doi:10.1038/s41467-019-09234-6
711

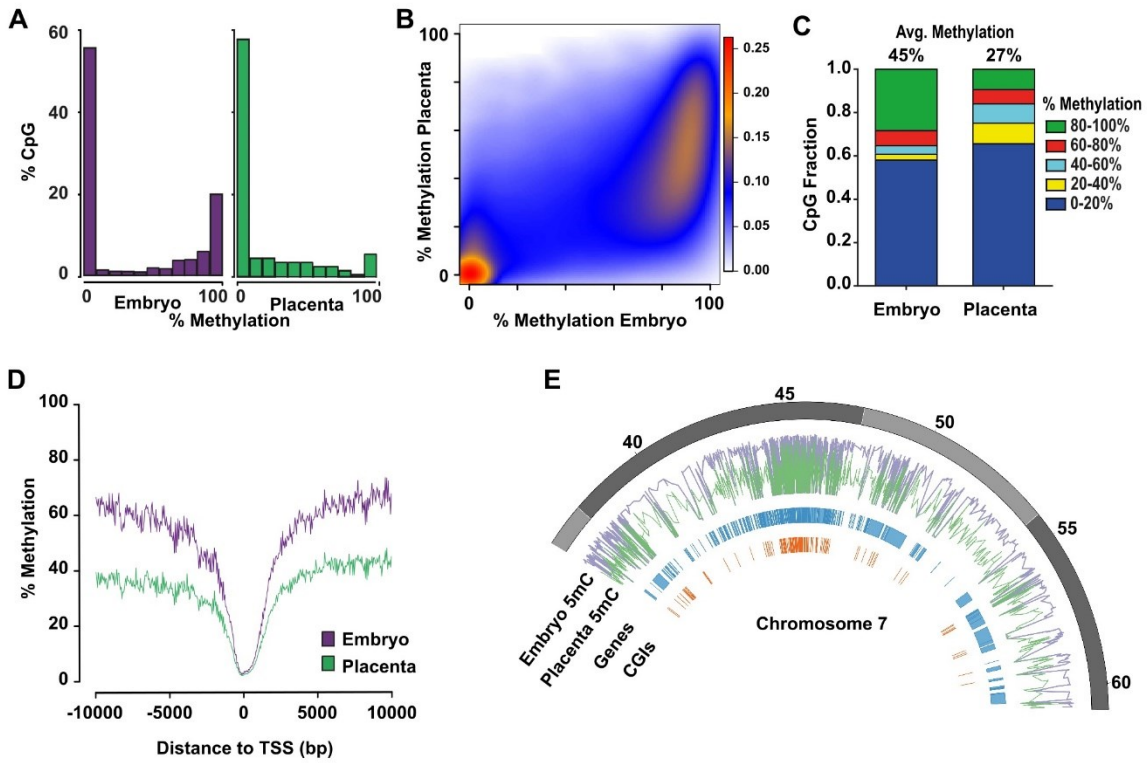

Figure 1. Distinctive patterns of genome-wide DNA methylation accumulation between E10.5 embryo and placenta. Analyses of genome-wide DNA methylation sequencing results for embryo (n=4) and placenta (n=4). **A)** Density histograms showing the distribution of CpG methylation levels for embryo (*purple*) and placenta (*green*). **B)** Pairwise comparison of CpG methylation between embryo and placenta. Density increases from blue to red. **C)** CpG fraction of 100 bp tiles within 0-20%, 20-40%, 40-60%, 60-80% and 80-100% ranges in embryo and placenta. Shown above bars, is the average CpG methylation for each unique tile represented in graph. **D)** DNA methylation means surrounding the transcription start site (TSS) for All-tiles in each experimental group. **E)** Circle plot showing methylation average of embryo (*purple*) and placenta (*green*) across a portion of chromosome 7.

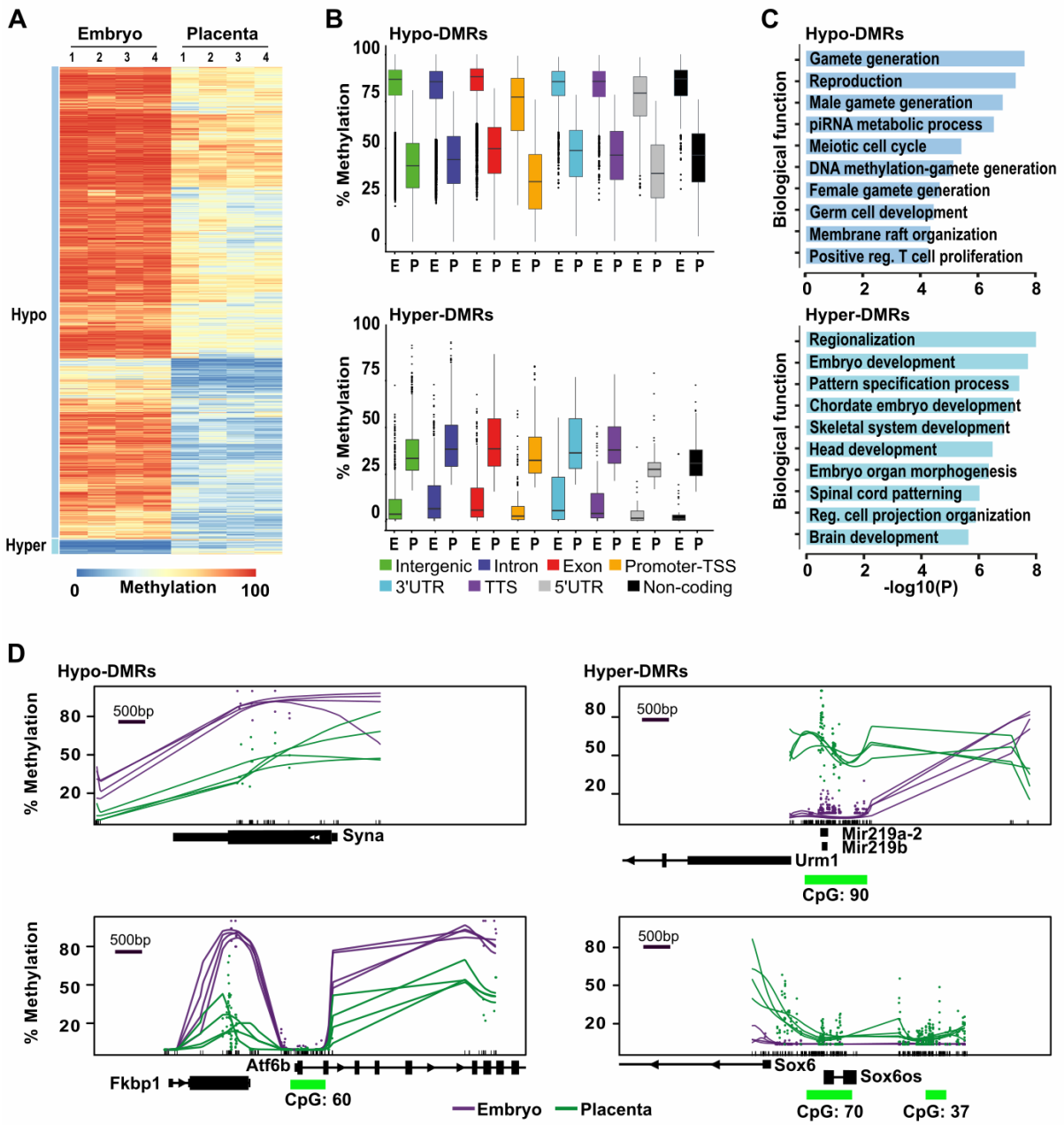

Figure 2. Genome-wide methylation asymmetry across genomic features between E10.5 embryo and placenta. Analyses of genome-wide DNA methylation sequencing results for embryo (n=4) and placenta (n=4) samples. **A)** Heatmap representation of DNA methylation levels for the 20 000 tiles with the most variable levels between embryo and placenta (DNA methylation variance >20% and $P<0.05$). **B)** Box-plots representing DNA methylation distribution in embryo and placenta for the different genomic annotation regions (intergenic, intron, exon, promoter-TSS, 3′UTR, TTS, 5'UTR and non-coding). **C)** Summary of biological functions associated with promoter regions in Hypo- and Hyper-DMRs. **D)** Examples of smoothed methylation profiles (*BSmooth* tool) in regions with lower methylation profiles (*Syna and Atf6b*) or higher methylation profiles (*Mir219a-2/Mir219b,* and *Sox6*) in placenta.

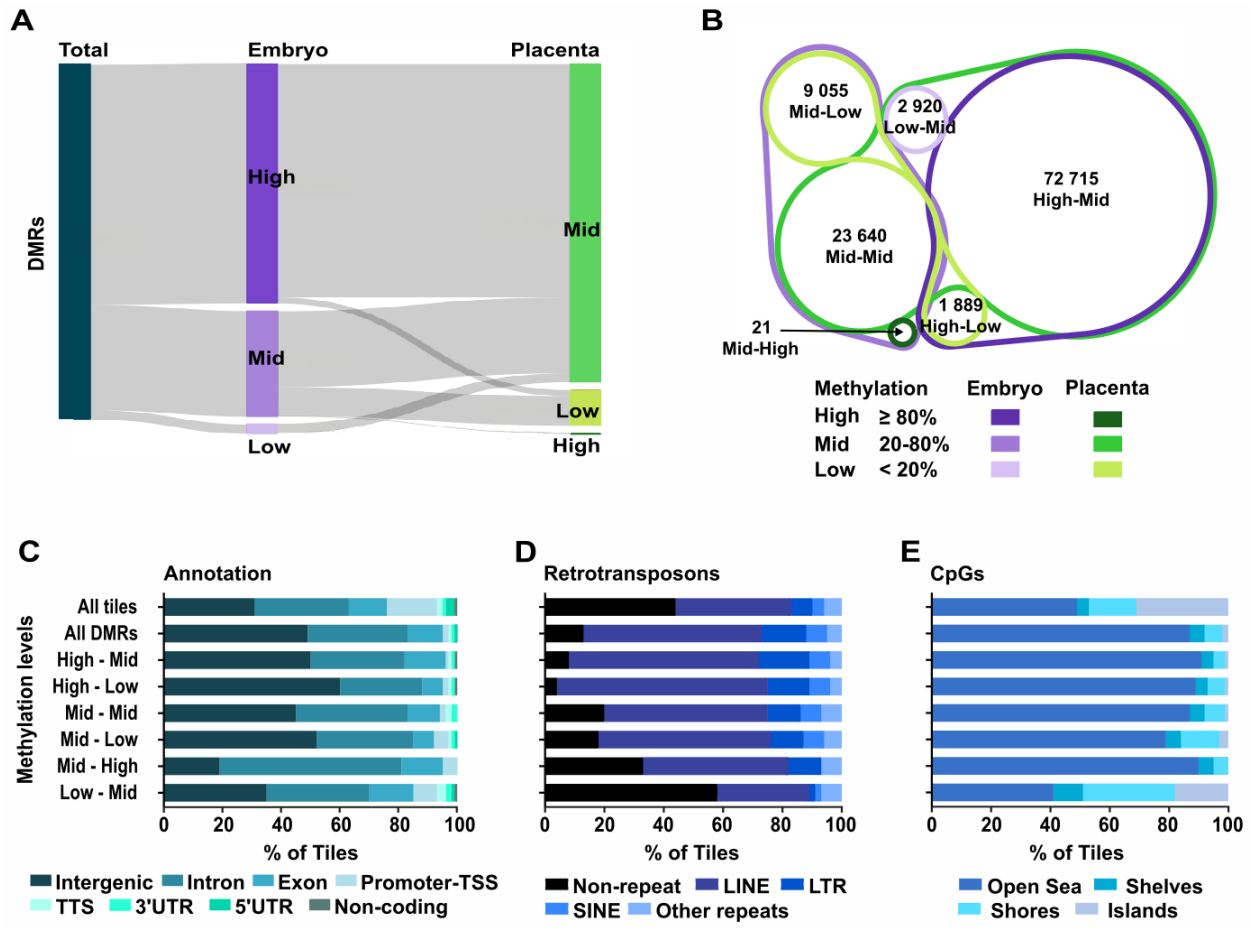

Figure 3. Distinct genomic features in DMRs based on their methylation status in E10.5 embryo and placenta. DMR analysis by methylation levels in embryo and placenta. **A)** Sankey diagram dividing DMRs by methylation levels in embryo (*purple*) and placenta (*green*) for the associated tiles. High : ≥80% methylation, Mid (intermediate) : ≥20% - <80% methylation , Low : <20% methylation. **B)** Venn diagram showing the proportion of tiles in the different DMR categories based on DNA methylation levels between embryo and placenta. **C), D)** and **E)** Analysis of all tiles, all the DMRs, as well as the 6 different DMR categories based on levels of DNA methylation in embryo and placenta for : **C)** Genomic annotations, **D)** Main retrotransposons and **E)** Proximity of CpG rich regions. Neighboring CpG dense regions were defined as shore; up to 2kb away from CGIs, shelf; 2-4kb away from CGIs, and open sea; >4kb away from CGIs.

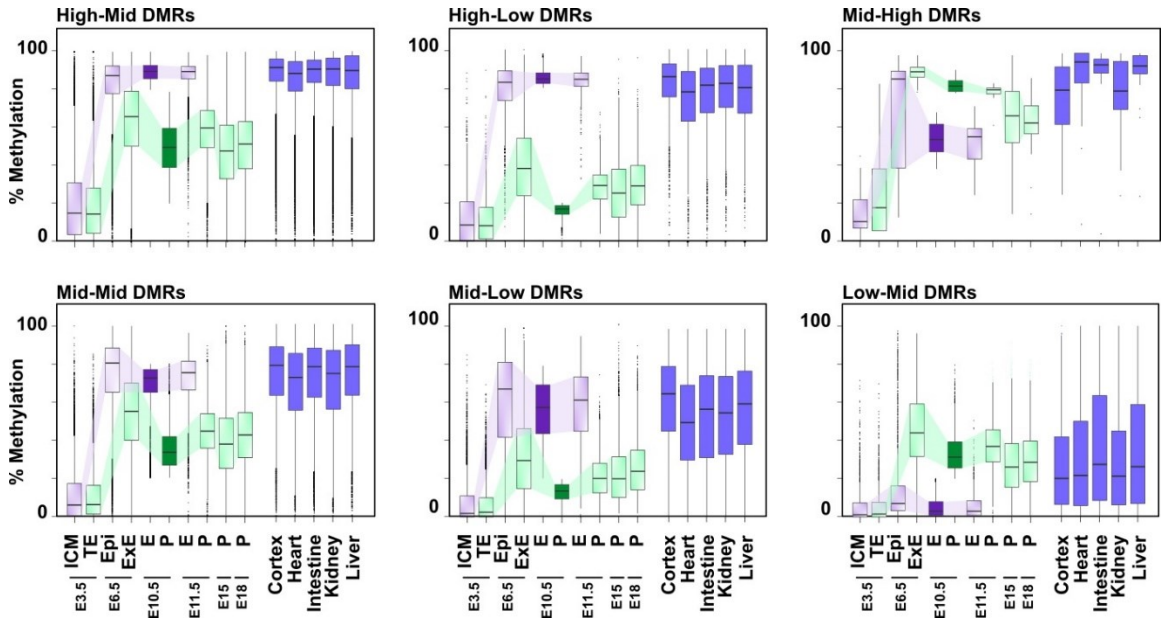

Figure 4. Dynamics of DNA methylation profiles associated with DMR categories and their evolution across embryo and placenta development. Box plots representing the DNA methylation distribution and median values for each DMR category in various developmental stages. Tiles associated with DMR categories at E10.5 were overlapped with previously published and publicly available data, and methylation levels were determined at each developmental stage (Smith et *al* 2012, Smith et *al*. 2014, Whidden et *al*. 2016) or in adult somatic tissues (Hon et *al*. 2013). ICM: inner cell mass, TE: trophectoderm, Epi: epiblast, ExE: extraembryonic ectoderm, E: embryo, Pla: placenta. See Table S2 for median and mean methylation values, and Table S4 for number of overlapping tiles analysed.

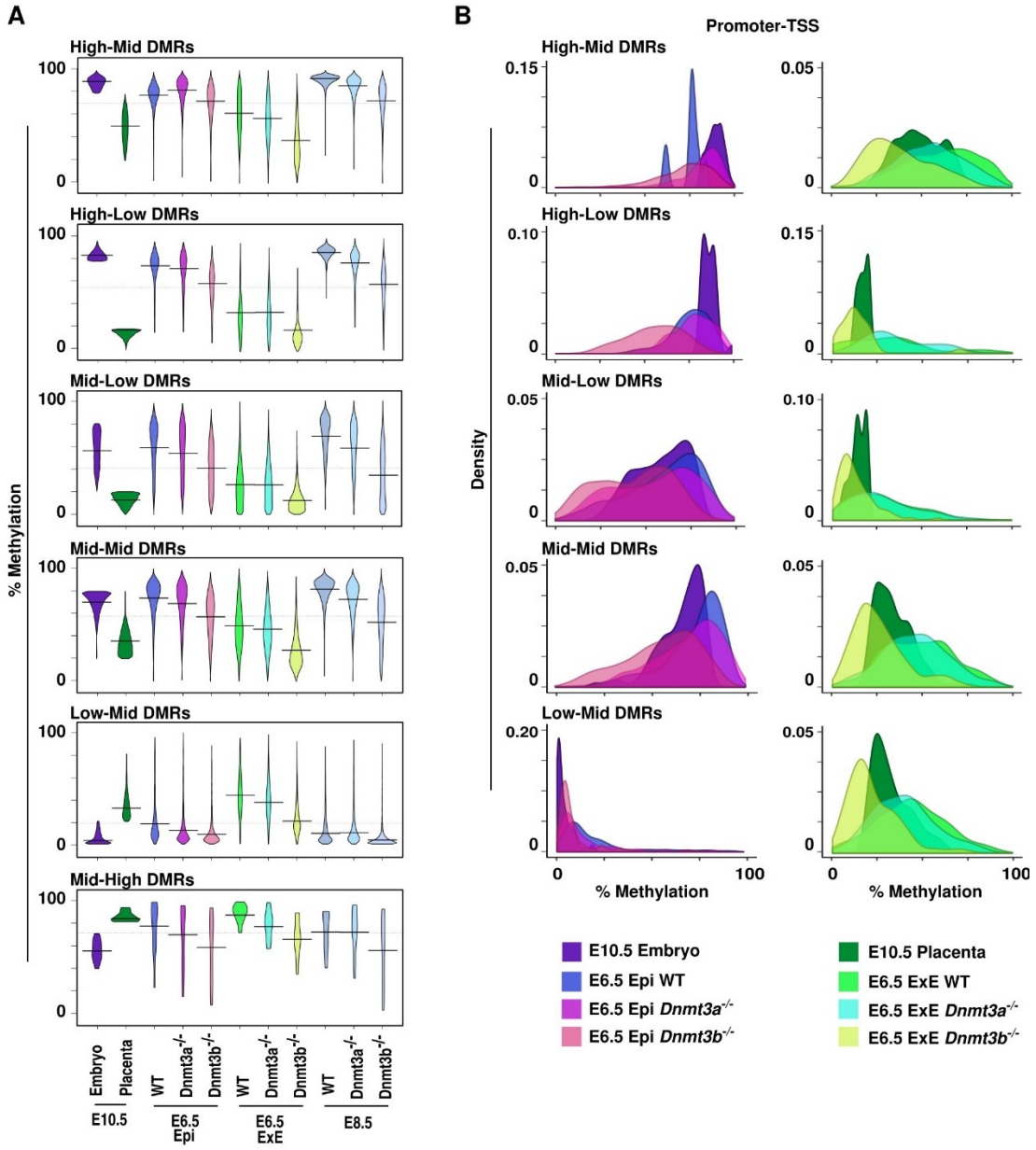

Figure 5. *Dnmt3a*- or *Dnmt3b*-deficiency alter proper establishment of DMR-associated patterns. A) Violin plot representing DNA methylation distribution and median values of tiles associated with the different DMR categories at E10.5, and their methylation levels in the different tissues and genotypes at E6.5 and E8.5. **B)** Promoter-TSS density graphs for E10.5 embryo and E6.5 epiblast (wt, *Dnmt3a*$^{-/-}$ and *Dnmt3b*$^{-/-}$) (left panel) and for E10.5 placenta and E6.5 extraembryonic ectoderm (wt, *Dnmt3a*$^{-/-}$ and *Dnmt3b*$^{-/-}$) (right panel). E: embryo, Epi: epiblast, ExE: extraembryonic ectoderm. See Table S3 for median and mean methylation values, and Table S4 for number of overlapping tiles analysed.

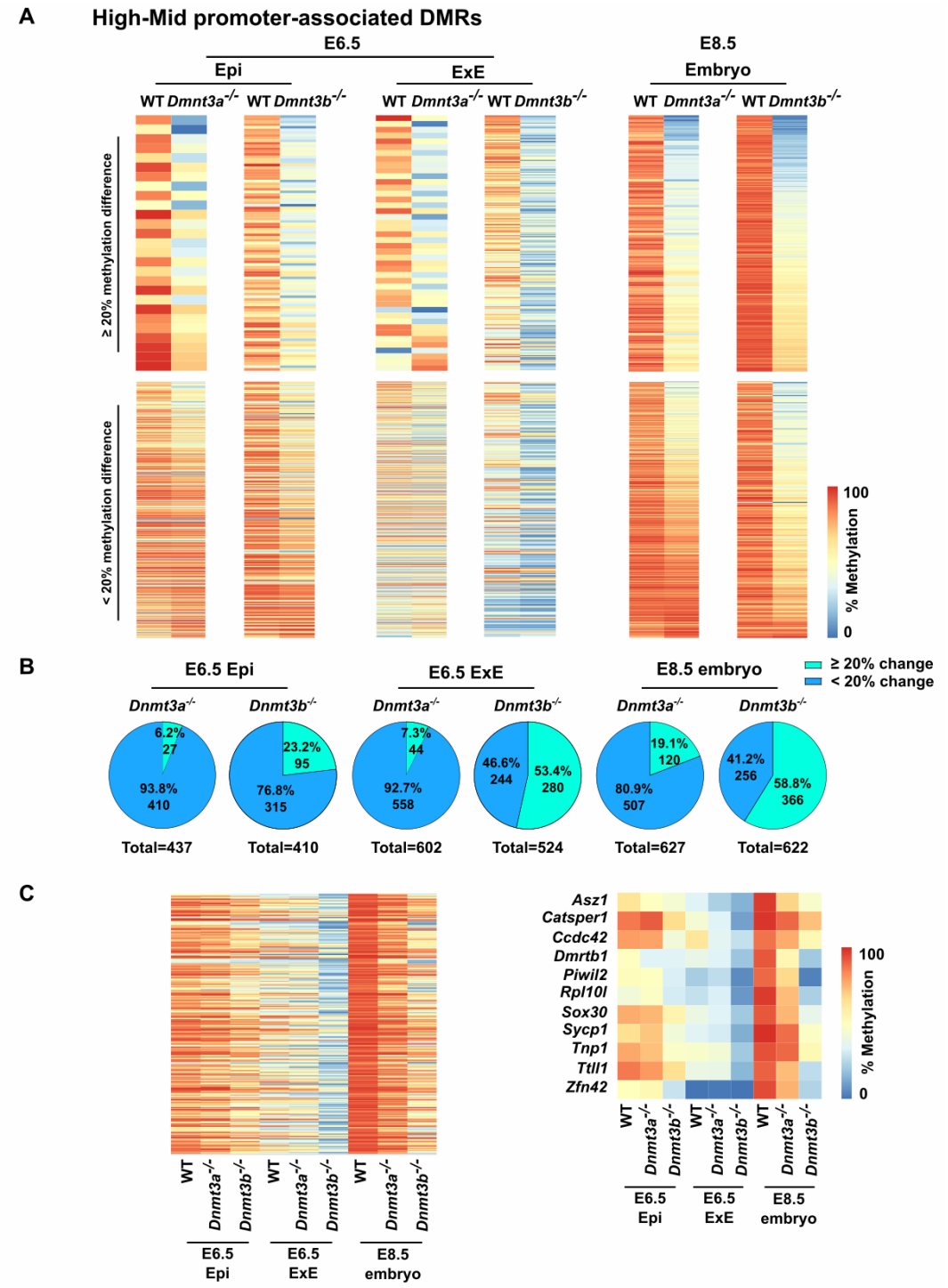

Figure 6. Developmental decline in compensatory DNA methylation mechanism in response to *Dnmt3a*- or *Dnmt3b*-deficiency at promoter-TSS associated with High-Mid DMRs. A) Heatmaps comparing the DNA methylation profiles of wt vs *Dnmt3a*$^{-/-}$ or wt vs *Dnmt3b*$^{-/-}$ for E6.5 epiblast, E6.5 extraembryonic ectoderm or E8.5 embryo in 100bp tiles overlapping promoter-associated DMRs that are highly methylated in the embryo (≥80%) and mildly methylated in the placenta (≥20 and <80%). Upper panel represents regions with a difference of methylation of at least 20% between wt and *Dnmt3a*$^{-/-}$ or wt and *Dnmt3b*$^{-/-}$. Lower panel represents stable regions

806 (lower than 20% difference in methylation). **B)** Pie charts representing DMR numbers for each
807 comparison. **C)** Heatmap of the methylation levels of tiles commonly represented in all 9 public
808 data samples that overlap with promoters-associated High-Mid DMRs (n = 314 tiles) (left panel).
809 Heatmap of the methylation level of gene associated with piRNA, gamete generation and germ
810 cells or meiotic nuclear division that are covered in all 9 public datasets (right panel).
811

812

813